

Should zeros count? Modeling the galaxy-globular cluster scaling relation with(out) zero-inflated count models

SAMANTHA C. BEREK ^{1,2,3,*} GWENDOLYN M. EADIE ^{1,4,3} JOSHUA S. SPEAGLE (沈佳士) ^{4,1,2,3} AND SHU YAN WANG ⁴

¹David A. Dunlap Department of Astronomy & Astrophysics, University of Toronto, 50 St George Street, Toronto, ON M5S 3H4, Canada

²Dunlap Institute for Astronomy & Astrophysics, University of Toronto, 50 St George Street, Toronto, ON M5S 3H4, Canada

³Data Sciences Institute, University of Toronto, 17th Floor, Ontario Power Building, 700 University Ave, Toronto, ON M5G 1Z5, Canada

⁴Department of Statistical Sciences, University of Toronto, 9th Floor, Ontario Power Building, 700 University Ave, Toronto, ON M5G 1Z5, Canada

ABSTRACT

The scaling relation between the size of a galaxy’s globular cluster (GC) population (N_{GC}) and the galaxy’s stellar mass (M_*) is usually described with a continuous, linear model, but in reality it is a count relationship that should be modeled as such. For massive galaxies, a negative binomial (NB) model has been shown to describe the data well, but it is unclear how the scaling relation behaves at low galaxy masses where a substantial portion of galaxies have $N_{GC} = 0$. In this work, we test the utility of Poisson and NB models for describing the low-mass end of the $N_{GC} - M_*$ scaling relation. We introduce the use of *zero-inflated* versions of these models, which allow for larger zero populations (e.g. galaxies without GCs) than would otherwise be predicted. We evaluate our models with a variety of predictive model comparison methods, including predictive intervals, leave-one-out cross-validation criterion, and posterior predictive comparisons. We find that the NB model is consistent with our data, but the naive Poisson is not. Moreover, we find that zero inflation of the models is not necessary to describe the population of low-mass galaxies that lack GCs, suggesting that a single formation and evolutionary process acts over all galaxy masses. Under the NB model, there does not appear to be anything unique about the lack of GCs in many low-mass galaxies; they are simply the low-mass extension of the larger $N_{GC} - M_*$ scaling relation.

1. INTRODUCTION

Globular clusters (GCs) provide a wealth of information about their host galaxies. Strong correlations exist between the mass (or number) of GCs in a galaxy and other properties such as galaxy halo mass, velocity dispersion, and black hole mass (e.g., Burkert & Tremaine 2010; Harris & Harris 2011; Harris et al. 2013, 2014; Forbes et al. 2018).

Beyond the Local Group, GC counts are often reported instead of more descriptive – but harder to measure – masses. Therefore, we have an acute interest in understanding the scaling relation between the *number* of GCs belonging to a galaxy (N_{GC}) and the galaxy’s other properties such as mass. These relationships are

often characterized using linear regression models meant for continuous response variables (e.g. Harris et al. 2013; Burkert & Forbes 2020). Count data are discrete, however, and a class of statistical models especially designed for these type of data exist. These models are a type of generalized linear model (GLM) that transform a continuous, linear response into a discrete one (see McCullagh & Nelder 1983, for a description of GLMs). Count models predict integer responses that match the data instead of un-physical responses such as fractions of counts. In particular, they perform far better than continuous models in the estimation of mean and variance in the low-count regime. Regression models for counts remain generally underused in astronomy, though, despite the prevalence of count data in a variety of fields (X-ray photons, neutrinos, planet counts, etc.).

de Souza et al. (2015a) introduced the use of count models for GC populations and found that, across a wide galaxy mass range, N_{GC} does not appear to be Poisson

Corresponding author: Samantha Berek
sam.berek@mail.utoronto.ca

* Data Sciences Institute Doctoral Student Fellow

distributed against a number of galactic predictor variables, but a negative binomial (NB) model fits the data and its dispersion well. Follow-up work on this topic has not yet been done, and the prevailing count distribution used for GC populations remains a Poisson.

Additionally, the mass scaling relation $M_* - M_{GC}$, which is well studied, can inform our choices of count models to explore. The $M_* - M_{GC}$ relation is linear for Milky Way-sized and larger galaxies, but becomes uncertain with a large dispersion for dwarfs (Harris et al. 2013; Bastian et al. 2020; Chen & Gnedin 2023). Scaling relations introduced by Eadie et al. (2022); Berek et al. (2023a) that include a zero-generating process in the form of a hurdle model were found to be good fits for the low-mass end of this scaling relation. Hurdle models are a form of GLM that combine a continuous response (for example, a linear regression) with a zero-generating process (i.e. a logistic regression). This allows for the modeling of a continuous population that includes zero values without needing to manually remove zeros and study them separately using occupation fractions. Therefore, it is worth investigating whether the same holds true for the low-number end of N_{GC} . This might point to the need for an associated physical process that creates large numbers of low-mass dwarfs without GC populations.

In this vein, we introduce the use of zero-inflated count models for GC count data for low-mass galaxies. Zero-inflated count models are similar to hurdle models in that they combine a count model with a separate zero-generating process. However, unlike hurdle models, the zeros in zero-inflated models can arise either from the zero-generating process or from the standard count model itself. The zero-generating process acts just to *increase* the total number of expected zeros, or galaxies without GCs. We investigate whether zero-inflation is necessary to model GC populations in low-mass galaxies and what this can tell us about the underlying processes of GC creation and destruction. We do this entirely in a Bayesian inference framework.

This paper is structured as follows: in Section 2, we describe our data. In Sections 3 and 4 we define our chosen count models (Poisson and negative binomial) and their zero-inflated counterparts, respectively. Section 5 introduces our inference methods. Section 6 explains our model evaluation procedures, and Section 7 presents our results. Section 8 ends with a summary and concluding remarks. Throughout, we use \ln to denote the natural logarithm \log_e , and \log to denote \log_{10} .

2. DATA

We use a compilation of three data sources with a focus on dwarf galaxies, originally compiled in Eadie et al.

(2022). The sample consists of Local Group galaxies, nearby dwarfs, and Virgo cluster galaxies. A summary of these data is presented here, but for further details, see Eadie et al. (2022).

The Local Group sample is an amalgamation of galaxy member lists from McConnachie (2012); Lim & Lee (2015); Simon (2019); Drlica-Wagner et al. (2020); Forbes (2020). The globular cluster information is taken from Harris et al. (2013); Lim & Lee (2015); Forbes et al. (2018); Forbes (2020). In total, the Local Group sample contains 100 galaxies, of which 20 have GC populations. This sample is the most complete in the universe due to our ability to image faint GC systems in our own Local Group.

The nearby dwarf galaxies, along with GC system masses, come from Georgiev et al. (2009, 2010). This sample consists of 39 galaxies, of which 31 have GCs. It focuses on isolated dwarfs outside of the Local Group.

The Virgo cluster survey is taken from Peng et al. (2008); Jordán et al. (2009). This sample consists of 93 galaxies with stellar masses $M_* < 10^{11} M_\odot$, all of which have GC systems. We use this sample to anchor the upper-mass end of our model, since the previous two samples contain far more low-mass galaxies than Milky Way-sized ones. We only include galaxies up to about the mass of the Milky Way, though, since we are focused on the low-mass end of the GC scaling relation.

Our data sample is plotted in Figure 1. The galaxies span the stellar mass range $10^3 < M_\odot < 10^{11}$, from ultra-faint dwarfs to Milky Way-sized galaxies. About a third of the galaxies do not have a GC system, while the rest do. However, there is a large galaxy mass range for which these two populations overlap.

3. COUNT MODELS

Count models are a class of generalized linear models (GLMs) that describe integer count data (see Nelder & Wedderburn 1972; McCullough & Nelder 1983; Gelman et al. 2013, for a discussion of GLMs). GLMs are linear in their parameters, but are mapped from this linear space to a different set via a link function $g(\mu)$ that transforms the mean response μ .

GLMs have been introduced in only a few astronomy contexts (in addition to those mentioned in Section 1), such as: modeling star formation and metal enrichment, and nuclear star cluster fractions, using binomial regression (de Souza et al. 2015b; Zanatta et al. 2021); photometric redshift estimation using gamma regression (Elliott et al. 2015); modeling ionizing radiation fractions using hurdle models with binomial and beta regression (Hattab et al. 2019); estimates of the dark matter field using negative binomial regression (Ata et al. 2015); and

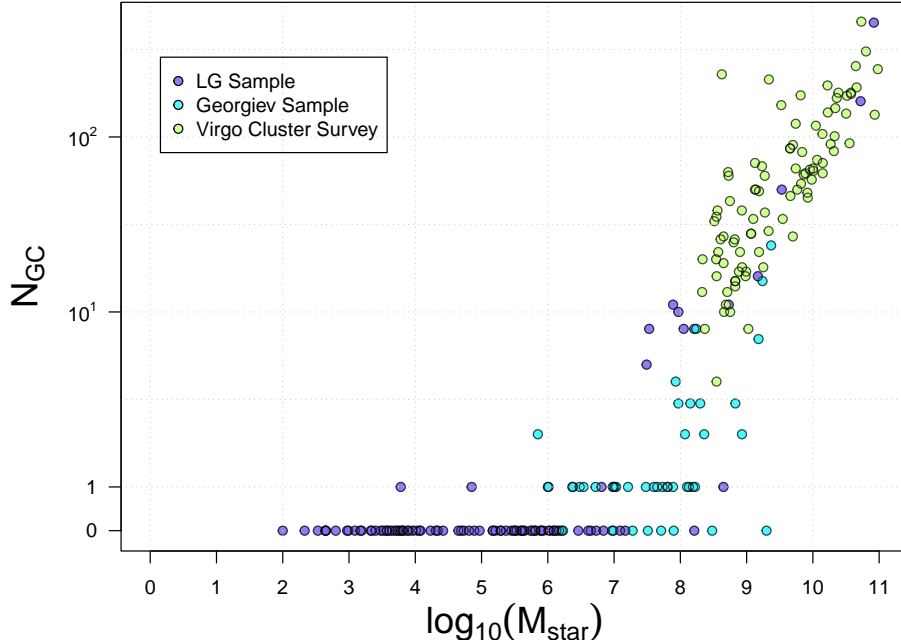


Figure 1. The number of GCs per galaxy, as a function of galaxy stellar mass, for our data. Points are colored according to the data source (i.e., Local Group sample, Georgiev sample, or Virgo Cluster Survey sample). The data consist of a large number of galaxies that do not have any globular clusters, as well as a substantial number of higher mass galaxies that have non-zero GC systems.

modeling galaxy cluster richness using Poisson regression (Andreon & Hurn 2010).

Here, we introduce two common count models: a Poisson model and a negative binomial model.

3.1. The Poisson model

The arguably simplest model for count data is the Poisson. The Poisson distribution describes the number of events that take place during some time period or within some spatial area, assuming independence between events and a constant mean rate of occurrence. It has only one parameter, λ , which describes both the mean and variance of the distribution. This implies that the mean is equal to the variance. In the context of galaxies and their GC populations, the number of GCs around a particular galaxy can be regarded as a realization of the random variable Y , which represents the number of events (GCs), given some predictor variable (in our case, log of galaxy stellar mass).

The probability mass function (PMF) $f(y)$ of the Poisson distribution gives the probability of count y , and is given by

$$f_P(y) = \frac{\lambda^y}{y!} \exp(-\lambda). \quad (1)$$

where $y = 0, 1, 2, \dots$. Here, we have introduced the subscript P to $f(y)$ denote the Poisson PMF.

To perform Poisson regression, the vector of means λ is related to a matrix of predictor variable(s) \mathbf{X} , called the design matrix¹, through a link function $g(\cdot)$:

$$g(\lambda) = \mathbf{X}\beta. \quad (2)$$

The vector λ is thus a linear combination of the predictor \mathbf{X} and a vector of coefficients β , which is then transformed through the link function. In our application, the design matrix \mathbf{X} is two columns wide: a column of 1s (for the intercept term) and a column for the covariate of galaxy stellar mass M_* . Thus, we fit a first-order linear combination: $g(\lambda_i) = \beta_0 + \beta_1 M_{*,i}$. The link function used for Poisson regression is the log link, such that $g(\lambda) = \ln \lambda$.

The likelihood for Poisson regression is based on the Poisson PMF. With $\lambda = \exp(\mathbf{X}\beta)$ and with some algebraic simplifications, this leads to the log-likelihood:

$$\ell_P(\mathbf{y}; \beta, \mathbf{X}) = \sum_{i=1}^n \left[(X_i \beta)^{y_i} - \exp(X_i \beta) - \ln(y_i!) \right]. \quad (3)$$

¹ This term comes from applied statistics. Each row in the design matrix is an observation. The first column of the matrix is a series of 1's (or 0's), indicating the inclusion (or not) of the intercept term in the model. The subsequent columns are the covariates/predictors/features.

In a standard Poisson distribution, the mean is equal to the variance (both are λ) — this is referred to as *equidispersion*. However, there are cases when the variance is higher or lower than the mean, which is called *overdispersion* and *underdispersion*, respectively. The overdispersion case is much more common than the underdispersion case. There exists a class of count models, called overdispersed Poisson models, that explicitly handle data that is Poisson overdispersed.

3.2. The negative binomial model

The negative binomial (NB) distribution is one of the most popular count models for overdispersed Poisson data. It is a mixture of Poisson and gamma distributions where the Poisson has a gamma-distributed mean. It therefore behaves similarly to a Poisson distribution, but also contains a second parameter to model variance.

There are multiple parameterizations of the NB model. We use the one described in Gelman et al. (2013). This parameterization has parameters λ and ϕ , which relate to the mean and variance as:

$$\begin{aligned} \mathbb{E}[Y] &= \lambda \\ \text{Var}[Y] &= \lambda + \frac{\lambda^2}{\phi}. \end{aligned} \quad (4)$$

In this parameterization, ϕ can be thought of as an “overdispersion” parameter that is inversely related to the variance. As ϕ decreases, the amount of extra dispersion compared to the Poisson dispersion λ increases, and is scaled by λ^2 . Often, ϕ is taken to be a constant that is not dependent on the predictor variables, but it can also be a linear function of the design matrix \mathbf{X} with the form $g(\phi) = \mathbf{X}\boldsymbol{\gamma}$.

The PMF of the NB model is

$$f_{\text{NB}}(y) = \left(\frac{(y + \phi - 1)!}{(\phi - 1)!y!} \right) \left(\frac{\lambda}{\lambda + \phi} \right)^y \left(\frac{\phi}{\lambda + \phi} \right)^\phi, \quad (5)$$

where $y = 0, 1, 2, \dots$

Similarly to Poisson regression, NB regression also uses a log link function for $\boldsymbol{\lambda}$. This leads to the log-likelihood function:

$$\begin{aligned} \ell_{\text{NB}}(\mathbf{y}; \boldsymbol{\beta}, \phi, \mathbf{X}) &= \sum_{i=1}^n \left[\ln [(y_i + \phi - 1)!] - \ln [(\phi - 1)!y_i!] \right. \\ &\left. + y_i X_i \boldsymbol{\beta} + \phi \ln(\phi) - (y_i + \phi) \ln [\exp(X_i \boldsymbol{\beta}) + \phi] \right], \end{aligned} \quad (6)$$

where we leave ϕ as a parameter that does not depend on the design matrix \mathbf{X} . However, if it does depend on \mathbf{X} , it is also transformed with a log link function $\ln(\phi) = \mathbf{X}\boldsymbol{\gamma}$ in the likelihood. We explore models both where ϕ is a constant and where it is a first order function of the predictors $\ln(\phi_i) = \gamma_0 + \gamma_1 X_i$.

4. ZERO-INFLATED COUNT MODELS

When a data set has an excess of zero values compared to that predicted by a Poisson, NB, or other model, the data is considered *zero-inflated*. Zero-inflated models describe scenarios where some of the zeros in a data set come from a process that also generates non-zeros (for example, a Poisson distribution), while others come from a separate process that only generates zeros.

A wide variety of models have zero-inflated counterparts. Here, we discuss the zero-inflated versions of the Poisson and NB models that were described in the previous section.

4.1. The zero-inflated Poisson model

The zero-inflated Poisson (ZIP) distribution was first described by Lambert (1992) and describes data for which there is an excess of zeros compared to a normal Poisson distribution. A ZIP model adds a Poisson PMF to a purely zero-generating process. This gives a mixture PMF of

$$f_{\text{ZIP}}(y) = \begin{cases} \pi_0 + (1 - \pi_0)f_{\text{P}}(y = 0|\lambda) & \text{if } y = 0 \\ (1 - \pi_0)f_{\text{P}}(y|\lambda) & \text{if } y > 0, \end{cases} \quad (7)$$

where $f_{\text{P}}(y)$ is the PMF of the Poisson distribution (Eq. 1) and π_0 is the fraction of excess zeros. Under this model, some of the zeros are from the Poisson distribution, while others are from the zero-generating process.

ZIP regression is similar to Poisson regression, also using the log link function for the mean parameter $\boldsymbol{\lambda}$. The zero-inflation parameter $\boldsymbol{\pi}_0$ can be decomposed as a linear function of the predictor $\boldsymbol{\pi}_0 = \mathbf{X}\boldsymbol{\eta}$, allowing the probability of excess zeros to depend on the predictor variable(s). The link function for the zero-inflated parameter is a logit, such that $\ln\left(\frac{\boldsymbol{\pi}_0}{1 - \boldsymbol{\pi}_0}\right) = \mathbf{X}\boldsymbol{\eta}$ (e.g., Yang et al. 2009; Campbell 2021). The (simplified) log-likelihood is therefore:

$$\ell_{\text{ZIP}}(\mathbf{y}; \boldsymbol{\beta}, \mathbf{X}, \boldsymbol{\eta}) = \begin{cases} \sum_{i=1}^n \left[\ln \left[\left(\frac{\exp(X_i \boldsymbol{\eta})}{1 + \exp(X_i \boldsymbol{\eta})} \right) (1 - \exp(-\exp(X_i \boldsymbol{\beta}))) + \exp(-\exp(X_i \boldsymbol{\beta})) \right] \right] & \text{if } y = 0 \\ \sum_{i=1}^n \left[\ln \left[\frac{1}{1 + \exp(X_i \boldsymbol{\eta})} \right] + \ell_{\text{P}}(y_i; \boldsymbol{\beta}, X_i) \right] & \text{if } y > 0. \end{cases} \quad (8)$$

4.2. The zero-inflated negative binomial model

The zero-inflated negative binomial (ZINB) distribution is an extension of the NB distribution in the same way that the ZIP distribution is an extension of the Poisson distribution. The ZINB distribution is a mixture of an NB with a zero-generating process, such that some zeros in the data come from the standard NB and others come from the zero process. The PMF is therefore:

$$f_{\text{ZINB}}(y) = \begin{cases} \pi_0 + (1 - \pi_0)f_{\text{NB}}(y = 0|\lambda, \phi) & \text{if } y = 0 \\ (1 - \pi_0)f_{\text{NB}}(y|\lambda, \phi) & \text{if } y > 0, \end{cases} \quad (9)$$

where π_0 is again the probability of excess zeros and $f_{\text{NB}}(y)$ is the PMF of the negative binomial distribution (Eq. 5). In regression, the parameters are transformed by a log link for λ (and ϕ if it is a function of \mathbf{X}), and a logit link for π_0 . The log-likelihood function for ZINB regression is then:

$$\ell_{\text{ZINB}}(\mathbf{y}; \boldsymbol{\beta}, \boldsymbol{\eta}, \phi, \mathbf{X}) = \begin{cases} \sum_{i=1}^n \left[\ln \left[\frac{\exp(X_i \boldsymbol{\eta})}{1 + \exp(X_i \boldsymbol{\eta})} \right] + \left(\frac{1}{1 + \exp(X_i \boldsymbol{\eta})} \right) \left(\frac{\phi}{\exp(X_i \boldsymbol{\beta}) + \phi} \right)^{\phi-1} \right] & \text{if } y = 0 \\ \sum_{i=1}^n \left[\ln \left[\frac{1}{1 + \exp(X_i \boldsymbol{\eta})} \right] \right] + \ell_{\text{NB}}(\mathbf{y}|\boldsymbol{\beta}, \phi, \mathbf{X}) & \text{if } y > 0. \end{cases} \quad (10)$$

Again, we leave ϕ as a parameter that does not depend on the predictors in Eq. 10. In a version where it is a function of \mathbf{X} , it must be transformed with the log link function $\ln(\phi) = \mathbf{X}\boldsymbol{\gamma}$ in the likelihood.

5. METHODS

We have chosen six different count models to test on our data set:

1. a Poisson
2. a zero-inflated Poisson (ZIP)
3. a negative binomial (NB)
4. an NB with a variable dispersion parameter (dependent on M_*)
5. a zero-inflated NB (ZINB)
6. a ZINB with a variable dispersion parameter (dependent on M_*).

Models with a non-constant dispersion parameter allow for different amounts of dispersion about the mean in different ranges of galaxy mass, which could correspond to the impacts of different physical processes acting on GCs in massive vs low-mass galaxies.

5.1. Inference

We use Bayesian inference for our modeling. Bayesian inference is based on Bayes' theorem, which states that

$$P(\theta|y) = \frac{P(y|\theta)P(\theta)}{P(y)}, \quad (11)$$

where θ are the model parameters and y are the data. $P(\theta|y)$ is the posterior, or the probability of a certain θ given y . $P(y|\theta)$ is the likelihood, $P(\theta)$ is the prior, and $P(y)$ is the evidence, which is a normalization term.

We do not have much physical intuition for the priors in these models. Therefore, we follow the example of [de Souza et al. \(2015a\)](#); [Eadie et al. \(2022\)](#) and use non-informative, broad priors. We choose the default priors in `brms` for each of the models, and data is centered before being fit.

All models are run using the R statistical software environment ([R Core Team 2021](#)) and the package `brms` ([Bürkner 2017](#)). The `brms` package compiles and runs Bayesian models in Stan ([Stan Development Team 2022a](#)), which is a Hamiltonian Monte Carlo (HMC) sampler ([Neal 2011](#); [Hoffman & Gelman 2011](#)). HMC algorithms are known to be more efficient than typical random walk samplers.

5.2. Measurement uncertainties

Ideally, one would include uncertainties for both galaxy stellar masses and GC counts in the analysis. Unfortunately, we do not have uncertainties for all of our data. While uncertainties on stellar masses are reported for the Local Group and Virgo samples, they are not reported for the Georgiev sample. Furthermore, none of the samples report uncertainties in GC counts, even though we expect uncertainties to exist. For example, we could be missing GCs that are located behind galaxy disks or that are fainter than detection limits, and counts could contain contamination from background galaxies in regimes where GCs appear as point sources (i.e. the Virgo sample).

While we could make some assumptions about the missing uncertainties and impute them, it is also not trivial to account for uncertainties in count models. Incorporating uncertainties in predictor variable(s) requires an errors-in-variables model, which adds N parameters to the fit (see [Berek et al. 2023a](#), for an example of errors-in-variables models in astronomy). Incorporating uncertainties in a count response variable relies

on an unknown PMF that includes selection effects and detection noise to link observed counts to true counts. This kind of uncertainty analysis is beyond the scope of this work and may require novel statistical methods. Thus, we leave this to future work and instead rely on the fact that our sample consists of nearby galaxies and thus we expect their GC data to be relatively complete. High levels of completeness are also suggested by two of our three data sources which have conducted completeness analyses on their samples (see Georgiev et al. 2009; Jordán et al. 2009, for details of their completeness analyses).

6. MODEL EVALUATION AND COMPARISON

There exist many methods to perform model comparison and evaluation. In astronomy, information criterion like the Akaike information criterion (AIC) and Deviance information criterion (DIC) are popular (Akaike 1973; Spiegelhalter et al. 2002). These methods give models a score based on the maximum likelihood estimate of the parameters (in AIC) for frequentist models, or based on the posterior mean point estimate of the parameters (in DIC) for Bayesian models. A fully Bayesian approach is the Watanabe-Akaike information criterion (WAIC), which computes the log average likelihood for each data point across the entire posterior distribution (Watanabe & Opper 2010). However, all of these methods rely on the maximum likelihood estimate or posterior of the model fit to the *original* data, instead of evaluating how well the model can *predict* additional data. The ability to accurately predict new data is a more philosophically Bayesian method of evaluating a model, and is practically useful in many astronomy cases, such as simulation building.

In this section, we describe multiple methods of predictive model comparison, which we will then apply on our models in Section 7. We use three different predictive methods that evaluate and compare models in different ways: (1) predictive intervals, which compare the intervals of real data to data simulated from our model; (2) leave-one-out cross validation, which compares the probability of a new, unseen data point across different models, and (3) a posterior predictive comparison, which evaluates the probability of the model itself.

6.1. Predictive Intervals

Predictive intervals show the range within which future data are expected to fall. This is different from a credible interval, which shows the range of uncertainty in the model parameters. Therefore, unlike credible intervals, predictive intervals provide an intuitive way of comparing not only the mean, or expectation value, of

the model, but also the dispersion about the mean. For example, if the model is a good description of the data, then we would expect roughly 75% of the data to fall within the 75% prediction interval.

6.2. Leave-one-out cross validation (LOO-CV)

LOO-CV (Vehtari et al. 2017) estimates the predictive abilities of a model on new data by removing one data point (y_i) and refitting the model to the $n-1$ remaining points (y_{-i}). It relies on the assumption that the fit to y_{-i} should be similar to the original fit to y , which allows for a predictive assessment without requiring additional data. LOO-CV calculates the expected log predictive density, or P_{y_i} , which is the probability of predicting the removed point y_i based on the fit to y_{-i} . This is analogous to the log likelihood, and is given by:

$$P_{y_i} = \sum_{i=1}^n \log p(y_i|y_{-i}) \quad (12)$$

for each removed data point y_i and remaining data y_{-i} on which the model is fit, where

$$p(y_i|y_{-i}) = \int p(y_i|\theta, y_{-i})p(\theta|y_{-i})d\theta \quad (13)$$

is the leave-one-out posterior predictive density for the y_{-i} data. To calculate a total LOO-CV value, the P_{y_i} for each removed point y_i are combined into a composite score.

P_{y_i} is a measure of how well the model can predict new data (y_i) that is not included in the model fit. A higher value indicates that more probability is concentrated at the unknown points y_i , making them more likely. However, these values are typically multiplied by -2 to follow the convention of other commonly used model comparison methods such as the AIC, DIC, and WAIC. Therefore, lower LOO-CV scores indicate better models.

6.3. Posterior Predictive Comparison

While LOO-CV is a useful model comparison method, it is only that. It can tell us which model is *best*, but not if that model is *good*. To evaluate whether any one model is consistent with the data, we use a posterior predictive check, which evaluates the likelihood of the posterior density instead of the comparing the likelihood of future data. To compute this posterior predictive, we do the following:

1. Randomly select one set of parameter values θ_i from the estimate of the posterior (i.e. the Markov chains).

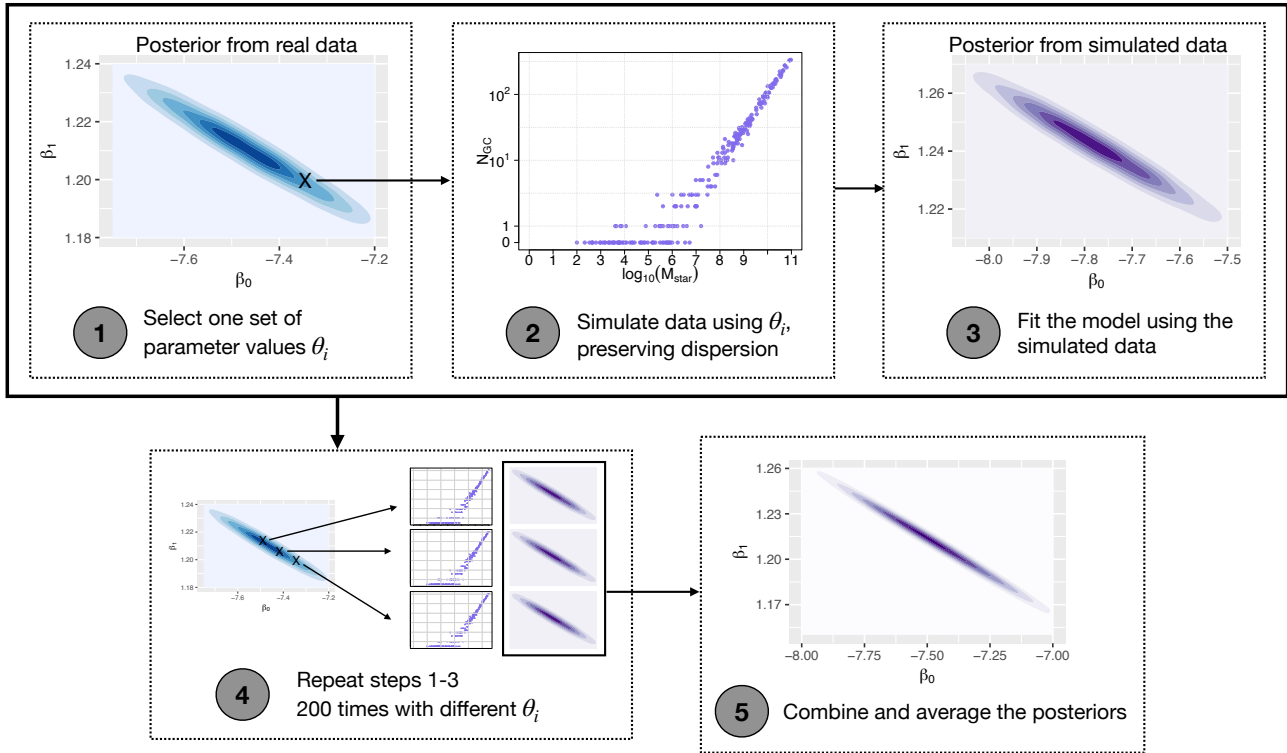


Figure 2. The process of computing the predicted range of posteriors for each model. A simple, two parameter model is illustrated here for visualization purposes. In step 1, one chain of the MCMC used to fit the real data to the model, with parameters θ_i , is selected. Next, we use the θ_i to simulate data with the same galaxy masses and dispersion as the original data. In step 3, we re-run the MCMC with this simulated data. We repeat this process 200 times with different chains θ_i and average the posteriors from the simulations. This gives the range of posteriors that are plausible for data that does fit the model, which can be compared to the posteriors from the fit with real data.

2. Given θ_i , simulate N_{GCS} for each M_* in our data set. Add random noise $\epsilon \sim N(0, \text{Var}(y))$ to N_{GCS} to mimic the dispersion of the data.
3. Re-fit the model with these simulated data, obtaining a new estimate of the posterior distribution and the associated posterior probability density.
4. Repeat steps 1-3 200 times. Combine the posterior samples and re-normalize to create a “global” posterior density.
5. Compare the “global” posterior density to the posterior density estimated from the observed data.

These steps to compute the predictive posterior are illustrated in Figure 2.

This predictive check provides a direct comparison between the “global” posterior density [i.e. the range of possible posteriors for data generated from a given model], and the posterior from our real data. If the posterior of our data falls within the range of expected posteriors, this indicates that our data is consistent with our model.

7. RESULTS

The estimated parameter values for each of the six models are listed in Table 1. To calculate estimates of the expectation value (mean), dispersion, and zero-inflation, the parameter values need to be transformed as indicated in Table 2, based on the link functions used for regression.

7.1. Predictive intervals

Predictive intervals for each of the six models are shown in Figure 3. The prediction intervals are, from outer to inner, 95%, 75%, and 50%. Black lines show the mean predictions, and purple points are our data.

Both versions of Poisson models shown in Figure 3 fail to capture the dispersion of the data, especially for larger galaxy masses. The ZIP model is better at predicting the mass range of galaxies without GCs, but both models do equally poorly at higher galaxy masses. All four versions of the NB model have much larger dispersions than the Poisson, especially at higher galaxy mass. The NB models with a dispersion parameter dependent on M_* have a dispersion that decreases with increasing galaxy mass. However, the varying disper-

Table 1. Posterior mean parameter values for each model.

Model Version	β_0	β_1	η_0	η_1	ϕ	γ_0	γ_1
Poisson	-7.46 (-7.72, -7.21)	1.21 (1.18, 1.24)	- -	- -	- -	- -	- -
ZIP	-6.92 (-7.20, -6.63)	1.16 (1.13, 1.19)	8.32 (5.20, 11.69)	-1.28 (-1.74, -0.87)	- -	- -	- -
NB	-10.35 (-11.57, -9.16)	1.52 (1.38, 1.65)	- -	- -	1.29 (1.00, 1.64)	- -	- -
NB (non-constant disp.)	-9.30 (-10.61, -7.90)	1.40 (1.25, 1.54)	- -	- -	- -	-4.19 (-6.41, -1.71)	0.49 (0.22, 0.73)
ZINB	-10.03 (-11.40, -8.65)	1.48 (1.33, 1.63)	1.51 (-10.18, 9.10)	-0.70 (-1.76, 0.49)	1.37 (1.04, 1.77)	- -	- -
ZINB (non-constant disp.)	-9.11 (-10.58, -7.66)	1.38 (1.23, 1.54)	1.11 (-9.45, 8.78)	-0.69 (-1.78, 0.50)	- -	-4.04 (-6.30, -1.66)	0.48 (0.22, 0.73)

NOTE—The values listed are the posterior means for each parameter of each model. The values in parentheses are the 95% credible intervals. Linear combinations of the above parameters, transformed by their respective link functions, provide estimates for the parameters λ , ϕ , and π_0 . See Table 2 for the equations needed to transform these fitted parameters into count estimates.

sion of these models do not significantly change the percentage of our data that fall within any of the intervals, compared to the non-variable dispersion case. The 95% predictive intervals, for example, cover about 95% of the data in all four of the NB models, meaning that they all seem capable of producing data similar to our galaxy sample.

7.2. LOO-CV

To more quantitatively assess model fit, we compare our six models using LOO-CV, which is computationally simple in `brms` and Stan using the `loo` package (Vehtari et al. 2023). As discussed in Section 6.2, lower values indicate a better model.

The LOO information criterion values for each model are listed in Table 3, along with their standard errors. The four versions of the NB model outperform the Poisson and ZIP. The differences between the various NB models, however, are indistinguishable given their standard errors. As discussed in Gelman et al. (2013), metrics like LOO-CV are only one tool in the model comparison and evaluation toolbox. Best practice suggests using multiple methods of model comparison and evaluation, along with physical intuition about the data and model choices, before coming to a conclusion.

7.3. Posterior Predictive Comparison

We follow the procedure described in Section 6.3 to perform a posterior predictive comparison, and plot the results in Figure 4. The “global” posterior densities from the simulated data tests (in purple) show the range of possible posteriors that would be expected from data that is consistent with the model. The posteriors from our data (in pink) are one realization, and thus expected to be much narrower than the simulated distribution. If the “global” and sample posterior distributions do not overlap, it indicates an unlikely sample posterior, i.e., that the data are not well fit to that model.

For the two Poisson distributions (first column in Figure 4), the posteriors from the real data are significantly different than the range of possible posteriors suggested by the simulated data. This suggests that our data is not Poisson distributed. The four NB posteriors of the real data, however, overlap with the distribution of simulated posteriors. This means that the data are consistent with the NB models. Similarly to the LOO-CV results, there are no distinguishing factors between the four NB models.

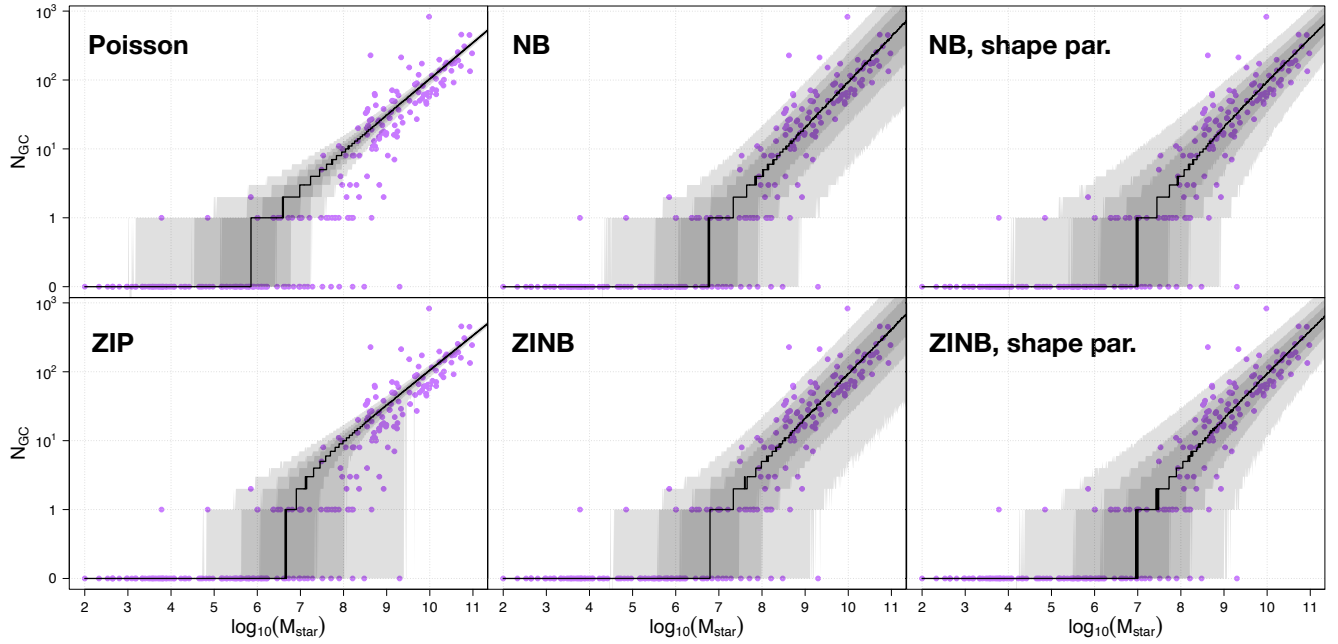


Figure 3. Predictive intervals for the six models. Shaded regions, from outer to inner, show the ranges in which 95%, 75%, and 50% of new data would be expected to lie. These regions should also encompass 95%, 75%, and 50% of the plotted galaxy data, if the given model is a good fit to the data.

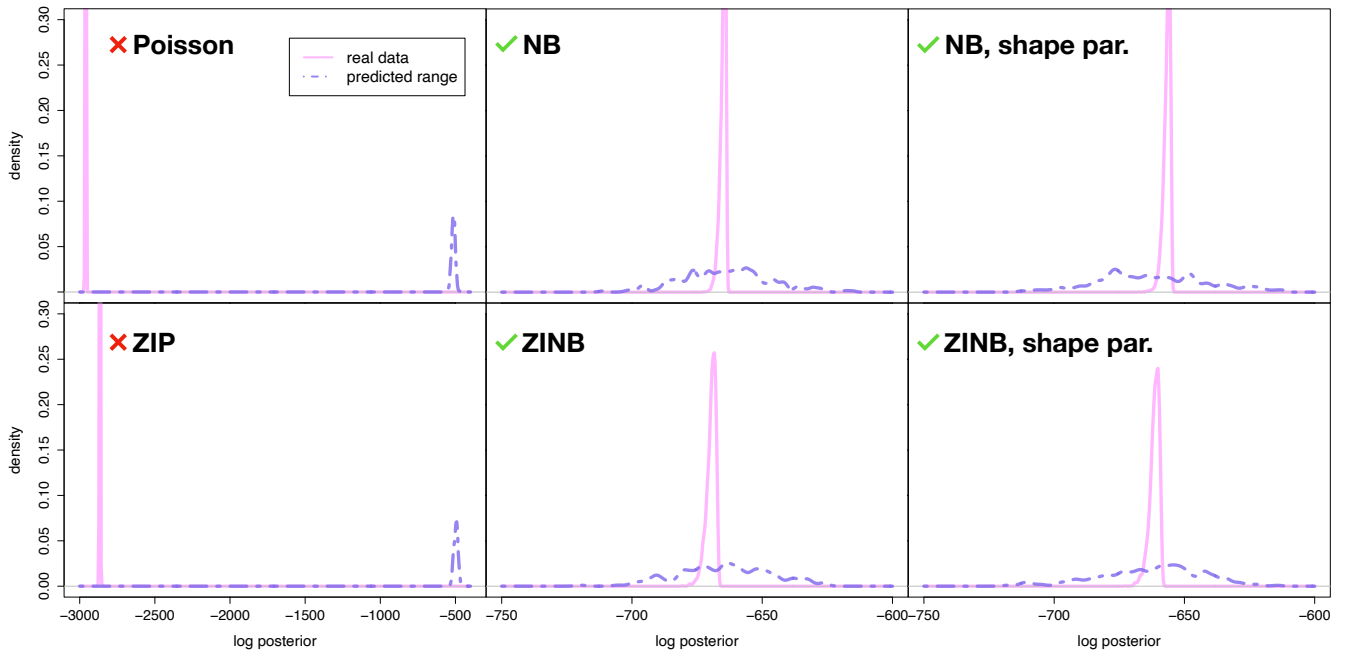


Figure 4. Posterior predictive comparisons for all six models. The solid pink posteriors are those from the real data fit to the model, and the dashed purple posteriors are the average from the posterior predictive check; i.e. the model run on data simulated from draws from the original posterior. Note: the y-axes are cut off at a density of 0.4 for visual clarity.

Table 2. How to use the values in Table 1.

	$E[N_m] = \lambda$	$\text{Var}[N_m] = SD[N_m]^2 = \lambda + \frac{\lambda^2}{\phi}$	π_0
	mean	variance	fraction of zero-inflation
Poisson	$\exp(\beta_0 + \beta_1 m)$	–	–
Example ($\log m = 10$)	104	–	–
ZIP	$\exp(\beta_0 + \beta_1 m)$	–	$\frac{\exp(\eta_0 + \eta_1 m)}{1 + \exp(\eta_0 + \eta_1 m)}$
Example ($\log m = 10$)	108	–	0.0112
NB	$\exp(\beta_0 + \beta_1 m)$	$\exp(\beta_0 + \beta_1 m) + \frac{(\exp(\beta_0 + \beta_1 m))^2}{\phi}$	–
Example ($\log m = 10$)	128	113^2	–
NB (non-constant disp.)	$\exp(\beta_0 + \beta_1 m)$	$\exp(\beta_0 + \beta_1 m) + \frac{(\exp(\beta_0 + \beta_1 m))^2}{\exp(\gamma_0 + \gamma_1 m)}$	–
Example ($\log m = 10$)	110	78^2	–
ZINB	$\exp(\beta_0 + \beta_1 m)$	$\exp(\beta_0 + \beta_1 m) + \frac{(\exp(\beta_0 + \beta_1 m))^2}{\phi}$	$\frac{\exp(\eta_0 + \eta_1 m)}{1 + \exp(\eta_0 + \eta_1 m)}$
Example ($\log m = 10$)	118	101^2	0.0041
ZINB (non-constant disp.)	$\exp(\beta_0 + \beta_1 m)$	$\exp(\beta_0 + \beta_1 m) + \frac{(\exp(\beta_0 + \beta_1 m))^2}{\exp(\gamma_0 + \gamma_1 m)}$	$\frac{\exp(\eta_0 + \eta_1 m)}{1 + \exp(\eta_0 + \eta_1 m)}$
Example ($\log m = 10$)	118	81^2	0.0030

NOTE—How to calculate the mean, variance, and zero-inflation for each model from the posterior mean values in Table 1. m refers to the log of the stellar mass for which a parameter value is to be calculated (i.e. $m = \log M_*$), and N_m refers to the number of GCs corresponding to the chosen m . The π_0 's for all models are poorly constrained (see the credible intervals in Table 1) and so the values calculated for the example are not considered robust.

Table 3. LOO-CV values for all models.

Model Version	LOO Information Criterion	Standard Error
Poisson	6046.4	2245.1
ZIP	5862.7	2208.0
Negative Binomial	1323.9	82.8
ZINB	1327.8	83.5
Negative Binomial (non-constant dispersion)	1318.1	83.4
ZINB (non-constant dispersion)	1321.3	84.1

NOTE—Smaller LOO information criterion values indicate more likely models.

8. DISCUSSION AND CONCLUSIONS

In this paper, we explore a variety of count models for use in GC counts of low-mass galaxies. We emphasize statistically robust methods of model comparison that are based in predictive methods, or the model’s ability to predict new data not used in model fitting. Our primary conclusions are as follows:

1. The GC populations of low-mass galaxies are not well described by a Poisson regression.
2. NB regressions are consistent with the GC data, and indicate greater variance (overdispersion) in GC counts as a function of galaxy mass than would be expected by a Poisson.
3. Zero-inflation is not necessary for GC populations, indicating a single process of GC formation over all galaxy masses.

These insights regarding our understanding of large star clusters in the smallest galaxies can provide important constraints in simulations and theoretical work on cluster and galaxy formation and evolutionary processes. They are described in more detail below, and we end with a look toward the future of this field.

8.1. *GC counts are not Poissonian*

The most simple count-generating process is a Poisson process, in which points are independently generated by sampling from a density distribution. Globular cluster counts have often been modeled with Poisson models before (e.g. Pfeffer et al. 2018; Huang & Kuposov 2021; Eadie et al. 2022). In their analysis, Eadie et al. (2022) presented evidence for the first time that the Poisson was a poor representation of the GC systems of low-mass galaxies. We come to a similar conclusion. The data do not match the Poisson prediction intervals, LOO-CV shows the Poisson models to be much worse than the negative binomials, and the predictive comparisons confirm that the Poisson models are not consistent with the data. This leads us to two possible interpretations: (1) if we believe that GCs should have originally formed around galaxies in numbers that followed a Poisson regression with respect to galaxy host mass, then our results indicate there are physical processes at play that cause deviations from the Poisson over time (i.e., cluster evolution), or, (2) perhaps GCs do not form around galaxies in numbers consistent with a Poisson regression to begin with.

A Poisson distribution is generated when events are sampled from the underlying density *independently*. However, this is clearly not the case with globular cluster formation. There is a finite amount of gas in a galaxy,

and when some of it is turned into a large star cluster, this removes that gas from the remaining gas that would be available to create more star clusters. This effect is more prominent in smaller galaxies, since they have less gas to begin with, and the formation of each large star cluster requires a larger percentage of the total gas in the galaxy. This galaxy-scale feedback from the formation of GCs violates the independence assumption of a Poisson distribution, making it an un-physical choice.

8.2. *An NB model provides insight for GC populations*

Just as de Souza et al. (2015a) found negative binomial models to be a better fit to GC count data for large galaxies, we find the same for low-mass galaxies. Our LOO-CV model comparison indicates that NB models are a far better choice than the Poisson for this data, and this is confirmed by our posterior predictive checks. Our data are consistent with multiple realizations of data drawn from the negative binomial model.

We began this model testing without much physical intuition for our models or priors. Our model comparison and predictive checks have informed us that NB models - but not Poisson models - are consistent with our sample of GCs of low-mass galaxies, which indicates that GC counts are overdispersed from a Poisson. The overdispersion corresponds to high variation in GC population size per galaxy mass.

The large dispersion in GC counts as a function of galaxy mass could be caused by other covariates, such as central black hole mass, velocity dispersion, halo mass, or star formation histories, that are absent in our model. Some of these covariates have been shown to correlate strongly with GC populations (e.g. Burkert & Tremaine 2010; Harris & Harris 2011; Harris et al. 2013, 2014; de Souza et al. 2015a; Forbes et al. 2018), although it is unclear whether their correlation to galaxy stellar masses or to GC populations is stronger. Some of the overdispersion could also be caused by stochastic processes or other confounding variables that have not yet been linked to GC populations.

Further factors, such as environment, could also impact the size of GC populations. This type of group-level effect could be incorporated into a model through the use of partial pooling or mixed models, which have the ability to fit for different values of parameters within different subsets of the data (i.e. isolated vs cluster galaxies). If group-level effects are important in this relationship, our ignoring of these effects would result in higher dispersion. Regardless of the cause of the overdispersion, however, we stress that the NB model is a good *empirical* model for the $M_* - N_{GC}$ relation. We leave

the exploration of other covariates and mixed models to future work.

8.3. Zero-inflation is not necessary for GC populations

Eadie et al. (2022) and Berek et al. (2023a) both showed that a significant portion of the lowest-mass galaxies do not have any GCs. Thus, we introduced zero-inflated versions of all of our models to allow for excess zeros. The posterior mean of the zero-inflation (π_0) parameter of the ZIP model approaches 1 in the lowest-mass regime and 0 in the higher mass regime ($\pi_0 = 0.87$ for $\log M_* = 5$ and 0.01 for $\log M_* = 10$), which indicates significant zero-inflation for the smallest galaxies, in line with expectations from other studies (e.g. Chen & Gnedin 2023; Berek et al. 2023a). However, the ZIP model’s LOO-CV score was equally as bad as that of the Poisson model. Therefore, we conclude that the π_0 parameter is attempting to compensate for the poor fit of the Poisson, rather than indicating a genuine need for a model with excess zeros. The zero-inflated NB models both have very poorly constrained π_0 parameters, and model comparison tests conclude that adding zero-inflation does not significantly improve the model fits. We operate under the philosophy that the simplest model that can adequately explain the data is the best one, and so we do not favor the zero-inflated (or variable dispersion NB) models over the simplest NB model.

Therefore, although there is an increasing proportion of galaxies that do not have GCs with decreasing mass, these galaxies seem to be the natural extension of one overall process of GC formation and evolution that operates over all galaxy masses. In other words, the same rules of GC formation and evolution seem to extend to all galaxies, regardless of their mass. This is an important result, not only for physical interpretation, but also for simulation studies; if one wishes to generate a realistic number of GCs around a simulated galaxy of a particular mass, then we recommend using our NB parameters to simulate that number of GCs, given the stellar mass of the host galaxy.

8.4. Looking to the future

The negative binomial model is consistent with the GC populations of nearby dwarf galaxies, but current GC counts in these galaxies are an amalgamation of the number of GCs that were originally formed and the number that have been completely disrupted due to mass-loss processes. GC formation and evolution are

governed by different physical processes happening over different timescales, and thus may not follow the same statistical models. If we could remove cluster evolution as a factor, perhaps by looking at nearby massive cluster formation (Berek et al. 2023b), newly formed GCs at high redshift in simulations such as E-MOSAICS and EMP-Pathfinder (Pfeffer et al. 2018; Reina-Campos et al. 2022), or younger GCs at high redshift with new telescopes like JWST (Mowla et al. 2022; Adamo et al. 2024), we could learn about cluster formation and evolution, and the statistical models that describe them, separately.

It remains to be seen what factors physically motivate an NB model. The open questions surrounding GC formation and evolution at high redshifts prevent us from choosing a model based purely off of physical intuition, and so we rely on the data to drive our model selection instead. The NB model, though, may yet inform our physical understanding of these processes. GC counts are often highly uncertain, especially at farther distances, due to background contamination and observational limits. Comparisons of NB models which are known to describe high-quality GC data to lower-quality data sets can provide information about clusters we are missing and further our understanding of large-scale GC properties and galaxy evolution.

ACKNOWLEDGEMENTS

The authors would like to thank the anonymous referee, whose comments greatly improved this manuscript. SCB would like to thank Steffani Grondin and Ayush Pandhi for helpful discussions throughout the writing of this manuscript. SCB is supported by the Data Sciences Institute at the University of Toronto through grant number DSI-DSFY3R1P24. GME acknowledges funding from NSERC through Discovery Grant RGPIN-2020-04554. JSS acknowledges funding from NSERC through Discovery Grant RGPIN-2023-04849. SYW was supported by the Summer Undergraduate Research Award (SURA) from the Department of Statistical Sciences, University of Toronto.

Software: Stan Modeling Language (Stan Development Team 2022a), R Statistical Software Environment (R Core Team 2022), and the following R packages: `rstan` (Stan Development Team 2022b), `loo`, Vehtari et al. (2022) `plotrix` (Lemon 2006), `ggplot2` (Wickham 2016), `bayesplot` (Gabry & Mahr 2022).

REFERENCES

- Adamo, A., Bradley, L. D., Vanzella, E., et al. 2024, arXiv e-prints, arXiv:2401.03224, doi: 10.48550/arXiv.2401.03224
- Akaike, H. 1973, Information theory and an extension of the maximum likelihood principle, 267–281

- Andreon, S., & Hurn, M. A. 2010, *MNRAS*, 404, 1922, doi: [10.1111/j.1365-2966.2010.16406.x](https://doi.org/10.1111/j.1365-2966.2010.16406.x)
- Ata, M., Kitaura, F.-S., & Müller, V. 2015, *MNRAS*, 446, 4250, doi: [10.1093/mnras/stu2347](https://doi.org/10.1093/mnras/stu2347)
- Bastian, N., Pfeffer, J., Kruijssen, J. M. D., et al. 2020, *MNRAS*, 498, 1050, doi: [10.1093/mnras/staa2453](https://doi.org/10.1093/mnras/staa2453)
- Berek, S. C., Eadie, G. M., Speagle, J. S., & Harris, W. E. 2023a, *ApJ*, 955, 22, doi: [10.3847/1538-4357/ace7b7](https://doi.org/10.3847/1538-4357/ace7b7)
- Berek, S. C., Reina-Campos, M., Eadie, G., & Sills, A. 2023b, *MNRAS*, 525, 1902, doi: [10.1093/mnras/stad2302](https://doi.org/10.1093/mnras/stad2302)
- Burkert, A., & Forbes, D. A. 2020, *AJ*, 159, 56, doi: [10.3847/1538-3881/ab5b0e](https://doi.org/10.3847/1538-3881/ab5b0e)
- Burkert, A., & Tremaine, S. 2010, *ApJ*, 720, 516, doi: [10.1088/0004-637X/720/1/516](https://doi.org/10.1088/0004-637X/720/1/516)
- Bürkner, P.-C. 2017, *Journal of Statistical Software*, 80, 1, doi: [10.18637/jss.v080.i01](https://doi.org/10.18637/jss.v080.i01)
- Campbell, H. 2021, *Methods in Ecology and Evolution*, 12, 665, doi: <https://doi.org/10.1111/2041-210X.13559>
- Chen, Y., & Gnedin, O. Y. 2023, *MNRAS*, doi: [10.1093/mnras/stad1328](https://doi.org/10.1093/mnras/stad1328)
- de Souza, R. S., Hilbe, J. M., Buelens, B., et al. 2015a, *MNRAS*, 453, 1928, doi: [10.1093/mnras/stv1825](https://doi.org/10.1093/mnras/stv1825)
- de Souza, R. S., Cameron, E., Killedar, M., et al. 2015b, *Astronomy and Computing*, 12, 21, doi: [10.1016/j.ascom.2015.04.002](https://doi.org/10.1016/j.ascom.2015.04.002)
- Drlica-Wagner, A., Bechtol, K., Mau, S., et al. 2020, *ApJ*, 893, 47, doi: [10.3847/1538-4357/ab7eb9](https://doi.org/10.3847/1538-4357/ab7eb9)
- Eadie, G. M., Harris, W. E., & Springford, A. 2022, *ApJ*, 926, 162, doi: [10.3847/1538-4357/ac33b0](https://doi.org/10.3847/1538-4357/ac33b0)
- Elliott, J., de Souza, R. S., Krone-Martins, A., et al. 2015, *Astronomy and Computing*, 10, 61, doi: [10.1016/j.ascom.2015.01.002](https://doi.org/10.1016/j.ascom.2015.01.002)
- Forbes, D. A. 2020, *MNRAS*, 493, 847, doi: [10.1093/mnras/staa245](https://doi.org/10.1093/mnras/staa245)
- Forbes, D. A., Read, J. I., Gieles, M., & Collins, M. L. M. 2018, *MNRAS*, 481, 5592, doi: [10.1093/mnras/sty2584](https://doi.org/10.1093/mnras/sty2584)
- Gabry, J., & Mahr, T. 2022, *bayesplot: Plotting for Bayesian Models*. <https://mc-stan.org/bayesplot/>
- Gelman, A., Carlin, J. B., Stern, H. S., & Rubin, D. B. 2013, *Bayesian data analysis*, 3rd edn. (Chapman and Hall/CRC)
- Georgiev, I. Y., Puzia, T. H., Goudfrooij, P., & Hilker, M. 2010, *MNRAS*, 406, 1967, doi: [10.1111/j.1365-2966.2010.16802.x](https://doi.org/10.1111/j.1365-2966.2010.16802.x)
- Georgiev, I. Y., Puzia, T. H., Hilker, M., & Goudfrooij, P. 2009, *MNRAS*, 392, 879, doi: [10.1111/j.1365-2966.2008.14104.x](https://doi.org/10.1111/j.1365-2966.2008.14104.x)
- Harris, G. L. H., & Harris, W. E. 2011, *MNRAS*, 410, 2347, doi: [10.1111/j.1365-2966.2010.17606.x](https://doi.org/10.1111/j.1365-2966.2010.17606.x)
- Harris, G. L. H., Poole, G. B., & Harris, W. E. 2014, *MNRAS*, 438, 2117, doi: [10.1093/mnras/stt2337](https://doi.org/10.1093/mnras/stt2337)
- Harris, W. E., Harris, G. L. H., & Alessi, M. 2013, *ApJ*, 772, 82, doi: [10.1088/0004-637X/772/2/82](https://doi.org/10.1088/0004-637X/772/2/82)
- Hattab, M. W., de Souza, R. S., Ciardi, B., et al. 2019, *MNRAS*, 483, 3307, doi: [10.1093/mnras/sty3314](https://doi.org/10.1093/mnras/sty3314)
- Hoffman, M. D., & Gelman, A. 2011, arXiv e-prints, arXiv:1111.4246, doi: [10.48550/arXiv.1111.4246](https://doi.org/10.48550/arXiv.1111.4246)
- Huang, K.-W., & Kuposov, S. E. 2021, *MNRAS*, 500, 986, doi: [10.1093/mnras/staa3297](https://doi.org/10.1093/mnras/staa3297)
- Jordán, A., Peng, E. W., Blakeslee, J. P., et al. 2009, *ApJS*, 180, 54, doi: [10.1088/0067-0049/180/1/54](https://doi.org/10.1088/0067-0049/180/1/54)
- Lambert, D. 1992, *Technometrics*, 34, 1
- Lemon, J. 2006, *R-News*, 6, 8
- Lim, S., & Lee, M. G. 2015, *ApJ*, 804, 123, doi: [10.1088/0004-637X/804/2/123](https://doi.org/10.1088/0004-637X/804/2/123)
- McConnachie, A. W. 2012, *AJ*, 144, 4, doi: [10.1088/0004-6256/144/1/4](https://doi.org/10.1088/0004-6256/144/1/4)
- McCullough, P., & Nelder, J. 1983, *Generalized Linear Models*, 2nd edn. (New York: Routledge)
- Mowla, L., Iyer, K. G., Desprez, G., et al. 2022, *ApJL*, 937, L35, doi: [10.3847/2041-8213/ac90ca](https://doi.org/10.3847/2041-8213/ac90ca)
- Neal, R. M. 2011, *MCMC using Hamiltonian dynamics*, ed. S. Brooks, A. Gelman, G. Jones, & X.-L. Meng (Chapman and Hall / CRC press)
- Nelder, J. A., & Wedderburn, R. W. M. 1972, *Journal of the Royal Statistical Society. Series A (General)*, 135, 370. <http://www.jstor.org/stable/2344614>
- Peng, E. W., Jordán, A., Côté, P., et al. 2008, *ApJ*, 681, 197, doi: [10.1086/587951](https://doi.org/10.1086/587951)
- Pfeffer, J., Kruijssen, J. M. D., Crain, R. A., & Bastian, N. 2018, *MNRAS*, 475, 4309, doi: [10.1093/mnras/stx3124](https://doi.org/10.1093/mnras/stx3124)
- R Core Team. 2021, *R: A Language and Environment for Statistical Computing*, R Foundation for Statistical Computing, Vienna, Austria. <https://www.R-project.org/>
- . 2022, *R: A Language and Environment for Statistical Computing*, R Foundation for Statistical Computing, Vienna, Austria. <https://www.R-project.org/>
- Reina-Campos, M., Keller, B. W., Kruijssen, J. M. D., et al. 2022, *MNRAS*, 517, 3144, doi: [10.1093/mnras/stac1934](https://doi.org/10.1093/mnras/stac1934)
- Simon, J. D. 2019, *ARA&A*, 57, 375, doi: [10.1146/annurev-astro-091918-104453](https://doi.org/10.1146/annurev-astro-091918-104453)
- Spiegelhalter, D. J., Best, N. G., Carlin, B. P., & Van Der Linde, A. 2002, *Journal of the Royal Statistical Society Series B: Statistical Methodology*, 64, 583
- Stan Development Team. 2022a, *Stan Modeling Language Users Guide and Reference Manual*, Version 2.31. <https://mc-stan.org/>

- . 2022b, RStan: the R interface to Stan. <https://mc-stan.org/>
- Vehtari, A., Gabry, J., Magnusson, M., et al. 2022, loo: Efficient leave-one-out cross-validation and WAIC for Bayesian models. <https://mc-stan.org/loo/>
- . 2023, loo: Efficient leave-one-out cross-validation and WAIC for Bayesian models. <https://mc-stan.org/loo/>
- Vehtari, A., Gelman, A., & Gabry, J. 2017, *Statistics and Computing*, 27, 1413, doi: [10.1007/s11222-016-9696-4](https://doi.org/10.1007/s11222-016-9696-4)
- Watanabe, S., & Opper, M. 2010, *Journal of machine learning research*, 11
- Wickham, H. 2016, *ggplot2: Elegant Graphics for Data Analysis* (Springer-Verlag New York). <https://ggplot2.tidyverse.org>
- Yang, Z., Hardin, J. W., & Addy, C. L. 2009, *Journal of Statistical Planning and Inference*, 139, 3340, doi: <https://doi.org/10.1016/j.jspi.2009.03.016>
- Zanatta, E., Sánchez-Janssen, R., Chies-Santos, A. L., de Souza, R. S., & Blakeslee, J. P. 2021, *MNRAS*, 508, 986, doi: [10.1093/mnras/stab2348](https://doi.org/10.1093/mnras/stab2348)